6756 *J. Org. Chem.* **1995**, *60*, 6756–6763

Nucleophilic Cleavage Products from *β*-Deprotonated Sesquidiazabicyclooctane Dication

Stephen F. Nelsen,*,† Hieu Q. Tran,† Randy K. Hiyashi,† Douglas R. Powell,† and
F. A. Neugebauer‡

*Department of Chemistry, University of Wisconsin, 1101 West University Avenue,
Madison, Wisconsin 53706-1396, and Abteilung Organische Chemie,
Max-Plank-Institut für medizinische Forschung, D-69028 Heidelberg, FRG*

Received July 5, 1995®

Nucleophilic cleavage of aminoaziridinium cation **2**$^+$ by PhS$^-$, N≡C$^-$, $CH_3CO_2^-$, and F$^-$ results in C–N$^+$ bond cleavage with inversion at carbon, producing essentially only the axially-substituted **3(X)** (<u>22/31</u>) derivatives for the latter two cases, but 40 and 15% exo-substituted **1(X)** (<u>22/22</u>) are initially produced for thiophenoxide and cyanide, respectively. The increase in oxidation potential for **3(CN)** vs **3** (0.22 V) is the same as that for replacement of the corresponding H by CN in an acyclic system. X-ray structures show that larger changes in nitrogen pyramidality ($\Delta\alpha_{av}$ +8.4 vs +5.8°) and NN distance (−0.172 vs −0.160 Å) occur upon electron loss from **3** than from **1**. Despite more constricted bond angles at nitrogen, crystalline **3**$^+$TsO$^-$ is more planar than **1**$^+$TsO$^-$ (α_{av} = 119.1° vs 118.6°), and the two double nitrogen inversion forms of **3**$^+$ are estimated to differ in energy by under 0.02 kcal/mol in solution from ENDOR and ESR studies. **3**$^{0/+}$ shows slower self-electron transfer than **1**$^{0/+}$ (k_{ex} (25 °C, CH_3CN) ~300 vs 700 M^{-1} s^{-1}). Neither more planar nitrogens for **3**$^+$ than for **1**$^+$ nor slower electron transfer for **3**$^{0/+}$ are predicted by AM1 calculations.

Introduction

Double oxidation of diazasesquibicylooctane **1** by nitrosonium cation gives the isolable dication **1**$^{2+}$ (see Scheme 1).[1] Deprotonation of **1**$^{2+}$ by pyridine or other difficultly oxidizable bases gives the thermally unstable aminoaziridinium cation **2**$^+$, which is reduced by borohydride to produce a mixture of the starting material **1** by cleavage of bond a and **3** by cleavage of bond b.[2] Where convenient, we will designate bis-*N*,*N*′-bicyclic hydrazines using the number of carbons in the bridges in addition to the two nitrogen bridge common to both bicyclic rings, so **1** is <u>22/22</u> and **3** is <u>22/13</u>. **1** is prepared by Diels–Alder addition of 1,3-cyclohexadiene to protonated 2,3-diazabicyclo[2.2.2]oct-2-ene followed by deprotonation and hydrogenation of the double bond,[1] and because 1,3-disubstituted six-membered rings are not available by Diels–Alder reactions, the 6,7-diazabicyclo[3.2.1]oct-6-ene required to make **3** by a proton-driven Diels–Alder reaction is not easily available, although it has been prepared.[3] Substituted bicyclic azo compounds or cyclic dienes can in principle be used for the Diels–Alder addition in preparing **1** derivatives, but in practice the necessity of protonating the azo compound before addition will occur makes the use of even rather weakly basic substituents impractical. The reactions shown in Scheme 1 are therefore an attractive way to prepare *γ*-substituted **1** and **3** molecules. In this work we examine the selectivity for cleavage of bonds a and b of **2**$^+$ by nucleophiles and determine how the geometries and the electron transfer thermodynamics and kinetics for **3**$^{0/+}$ compare with **1**$^{0/+}$ and how they are affected by changing substituents X.

Scheme 1

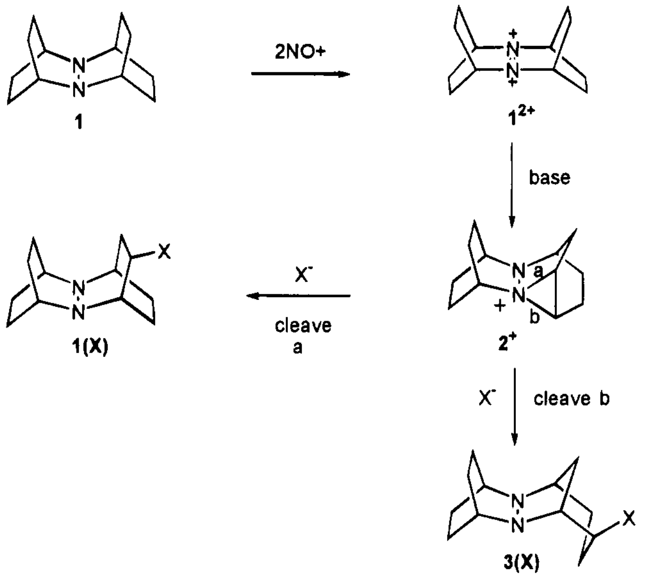

Results and Discussion

Cleavage of 2 to Substituted 1 and 3. A 1.8/1 ratio of **3**/**1** was produced from **1**$^{2+}$ by deprotonation with pyridine at low temperature and reduction with tetramethylammonium borohydride,[2] but later experiments showed that this does not accurately reflect the selectivity for hydride cleavage of the two C–N$^+$ bonds present in **2**$^+$. When other nucleophiles are employed, we usually get about 10–15% recovered neutral **1**, which probably arises from incomplete deprotonation of **1**$^{2+}$ and reduction of **1**$^{2+}$ to **1** by the nucleophile. Reaction of **2**$^+$ with nucleophiles produces single diastereomers of 4-substituted **3(X)** and **1(X)**, as shown by the ^{13}C-NMR spectra of these products having only a single set of peaks. It is easy to tell from ^{1}H-NMR studies that this diastereomer is the 4-axial-substituted compound for **3(X)**. This was also demonstrated by the crystal structure obtained for **3(OAc)**. The thermal ellipsoid drawing of Figure 1 shows

---

† University of Wisconsin.

‡ MPI Heidelberg.

® Abstract published in *Advance ACS Abstracts*, September 15, 1995.

[1] (a) Nelsen, S. F.; Blackstock, S. C.; Frigo, T. B. *J. Am. Chem. Soc.* **1984**, *106*, 3366. (b) Nelsen, S. F.; Blackstock, S. C.; Frigo, T. B. *Tetrahedron* **1986**, *42*, 1769.

[2] Nelsen, S. F.; Wang, Y. *J. Am. Chem. Soc.* **1991**, *113*, 5905.

[3] Wilson, R. M.; Rekers, J. W. *J. Am. Chem. Soc.* **1979**, *101*, 4005.

0022-3263/95/1960-6756$09.00/0

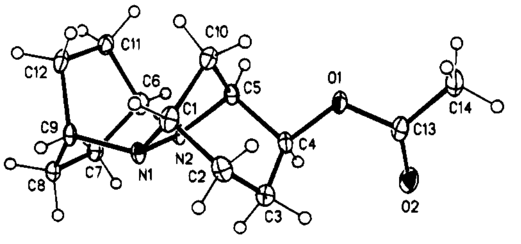

Figure 1. Thermal ellipsoid (50%) drawing of the X-ray structure of **3(OAc)**.

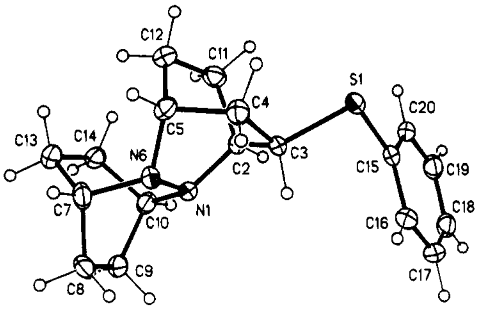

Figure 2. Thermal ellipsoid (50%) drawing of the X-ray structure of **1(SPh)**.

Table 1. Regioselectivity for Nucleophilic Cleavage of 2^+ Generated by Pyridine Deprotonation of 1^{2+}

		rel fractions[a]		
nucleophile	X	crude yield, %	**3-X**	**1-X**
Na^+PhS^-	SPh	95	0.60	0.40
$Bu_4N^+CN^-$	CN	102	0.85	0.15[b]
$Et_4N^+AcO^-{\cdot}H_2O$	OAc	99[c]	>0.95	unobsd
$BnMe_3N^+F^-{\cdot}H_2O$	F	53[d]	>0.95	unobsd

[a] Estimated by NMR integration on the reaction product. [b] Fractions estimated after removal of **1** by crystallization. [c] Assuming 16.7% of the material was **1**, as estimated by NMR. [d] Assuming 39% of the crude material was **1**, as estimated by NMR. In some experiments, a small amount of material which might be **1-F**, oxidizing at about −0.42 V vs SCE, was detected by cyclic voltammetry. In most experiments significant amounts of this material were not found.

that it crystallizes in the double nitrogen inversion form (invertomer) having the one carbon bridge of the 13 ring *syn* to a two carbon bridge of the 22 ring, which we will abbreviate as **1s2**, and with the 1,3-substituted cyclohexane ring in a chair form having the acetyl substitutent axial, as shown in Scheme 1. It is more difficult to determine the stereochemistry of **1(X)** from NMR studies, but the X-ray structure of **1(SPh)** (Figure 2) demonstrates that the substituent is *exo*, as shown in Scheme 1, and that it crystallizes in the invertomer with the substituent on an "outer" methylene group instead of that shown in Scheme 1, which has the substituent on an "inner" methylene group; the two should be very similar in energy. It may be noted that both **1(X)** and **3(X)** are formed with inversion of stereochemistry at the carbon being substituted, which is consistent with S_N2 attack of the nucleophile at the $C{-}N^+$ bonds of 2^+.

Table 1 shows the results of experiments using thiophenoxide, cyanide, acetate, and fluoride as nucleophiles to cleave 2^+ generated from 1^{2+}. The neutral hydrazine mixture was isolated by pentane extraction after the reaction mixture was allowed to warm to room temperature, and the relative amounts of **3(X)** and **1(X)** were determined by NMR integration. **1(X)** is clearly formed when PhS^- and CN^- are used as nucleophile, but little or none could be detected using the harder nucleophiles AcO^- and F^-. A significant amount of water was present in the latter two cases, although **3(OH)** was not detected. **1(X)** and **3(X)** might interconvert by ionization of **3(X)** to a $2^+,X^-$ ion pair, followed by readdition of X^-, but this does not appear to occur, even under conditions harsher than those used. The relative amounts of **3(SPh)** and **1(SPh)** changed less than 1% after heating at 60 °C for 30 h in acetonitrile, and heating **3(OAc)** with Me_4NCN in acetonitrile at 60 °C for 43 h resulted in no formation of either **3(CN)** or **1(CN)**. If $2^+,OAc^-$ ion pairs are formed, they do not exchange acetate for cyanide present in the solution. These experiments suggest that the relative amounts of **3(X)** and **1(X)** observed represent a kinetically controlled product mixture, and we have written the nucleophilic additions to 2^+ in Scheme 1 as irreversible reactions.

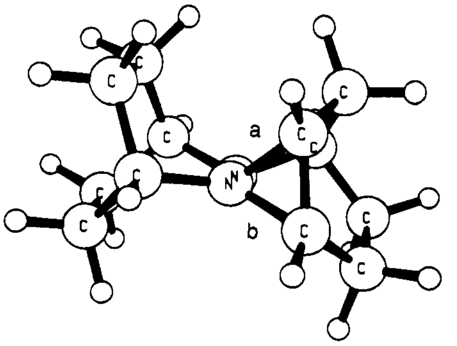

Figure 3. Ball and stick drawing of the AM1 minimum energy structure of **2**.

Nucleophilic attack at the $C{-}N^+$ bond adjacent to the two atom bridge of 2^+ (bond b in Scheme 1) to give **3(X)** derivatives is significantly faster than that at bond a. One would expect the relative energies of the transition states to reflect the exothermicities of the reactions, but these exothermicities appear to be close for relaxed **1** and **3**. AM1 calculations get **1** and **3** to be almost equal in energy, with **3** 0.4 kcal/mol less stable than **1**. We suggest that the observed predominance of **3(X)** over **1(X)** results from a stereoelectronic effect. The nitrogen inversion form of 2^+ shown in Scheme 1 has the one-carbon bridge of its tricyclic half *syn* to the 22 ring (a drawing of the AM1 structure shown as Figure 3) and is calculated by AM1 to be 7.5 kcal/mol more stable than the trivalent nitrogen inversion conformation, which has the two carbon bridge of the tricyclic half *syn* to the 22 ring. We presume that the form shown in Figure 3 is that attacked by X^-. A steric approach argument does not appear to favor cleavage of bond b; we would expect cleavage of bond a, next to the one carbon bridge, to also be sterically more favorable. Trisubstituted nitrogen lone pair, $\sigma(N^+{-}C)$ interaction ought to weaken the $N^+{-}C$ bonds, and bond b is calculated to have significantly poorer lp,$C{-}N^+$ overlap than bond a: the $CN^+,N'lp$ twist angle χ of 65.7° is calculated for bond b versus 130.0° for bond a, $\cos^2 \chi$ values 0.17 and 0.41, respectively. Although the $N^+{-}C$ bonds will be bent, bond a will clearly have better lp,$\sigma(N^+C)$ overlap than b. Because lp,$C{-}N^+$ interaction will tend to lower polarization of the $N^+{-}C$ bond, greater interaction for bond a might favor nucleophilic attack at the carbon of bond b. We suggest, however, that the principal reason for bond b cleavage being favored is that an unfavorable conformation of **1(X)** is initially produced if bond a cleavage occurs. It can be noted from Figure 3 that the $N{-}N^+{-}C_\alpha$ plane, where C_α is the attached bridgehead carbon in the 22 ring, approximately bisects the aziridinium ring and that the lone pair at the trisubstituted nitrogen is directed down

Table 2. Oxidation Potentials[a] of 1-X and 3-X

	1-X		**3-X**	
X	$E^{\circ\prime}$ (ΔE_p)[b]	$\Delta\Delta G^{\circ c}$	$E^{\circ\prime}$ (ΔE_p)[b]	$\Delta\Delta G^{\circ d}$
H	-0.52_9 (0.07)	≡0	-0.16_4 (0.10)	≡0[e]
SPh	-0.42_4 (0.08)	+2.4	-0.05_6 (0.07)	+2.5
OAc			-0.06_5 (0.11)	+2.3
F			-0.00_8 (0.09)	+3.6
CN	-0.34_6 (0.07)	+4.2	$+0.05_9$ (0.07)	+5.1

[a] In acetonitrile containing 0.1 M tetraethylammonium perchlorate, potentials reported in V vs a standard calomel electrode. [b] Using $E^{\circ\prime} = (E_p^{ox} + E_p^{red})/2$; numbers in parentheses are $\Delta E_p = E_p^{ox} - E_p^{red}$. [c] $\Delta\Delta G^\circ$ (kcal/mol) = 23.06[$E^{\circ\prime}$(**1-X**) − $E^{\circ\prime}$(**1-H**)]. [d] $\Delta\Delta G^\circ$ (kcal/mol) = 23.06[$E^{\circ\prime}$(**3-X**) − $E^{\circ\prime}$(**3-H**)]. [e] $E^{\circ\prime}$(**3-H**) − $E^{\circ\prime}$(**1-H**) is $+0.36_5$ V = +8.4 kcal/mol.

in this view. Cleavage of bond b initially produces the more stable *syn* lone pair form of **3(X)**, while cleavage of bond a should initially give the considerably destabilized[4] *anti* lone pair nitrogen inversion form of **1(X)**.[5] This difference in initial product stabilities should be partially reflected in the relative energies of the transition states. It may be noted from Table 1 that the softer nucleophiles CN^- and PhS^- give significantly more **1(X)** than do F^- and OAc^-. This would not be the result if size of the nucleophile were important in determining the product ratio. The reactions of 2^+ with CN^- and PhS^- are noticably faster than those with the harder nucleophiles F^- and OAc^-, as expected for S_N2 reactions. By Hammond's postulate, the slower reactions with the harder nucleophiles should have later transition states, which is consistent with the greater predominance of **3(X)** which is observed in these reactions.

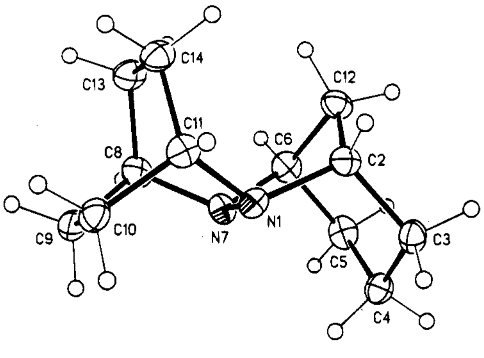

Figure 4. Thermal ellipsoid (35%) drawing of the X-ray structure of **3**.

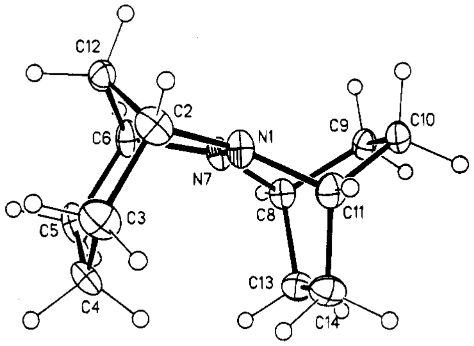

Figure 5. Thermal ellipsoid (50%) drawing of the X-ray structure of 3^+.

Ease of Oxidation of 3 vs 1. Table 2 contains electrochemical data for **1**, **3**, and their derivatives. The 31 ring present in **3** restricts the NNC angles relative to **1**, which is expected to make flattening at nitrogen more difficult and raise the formal potential for oxidation, $E^{\circ\prime}$. This effect is rather large, and **3** is 8.4 kcal/mol (0.365 V) harder to oxidize than is **1**. The more difficult oxidation for **3** than **1** is successfully predicted by AM1 calculations, which get $\Delta\Delta H_f$ for $3^{0/+}$ to be 9.4 kcal/mol (0.40 V) larger than for $1^{0/+}$. Substitution by γ-SPh and -OAc raises $E^{\circ\prime}$ by 2.3−2.5 kcal/mol, which is about the same amount as does the introduction of a γ double bond in **4**. The more electron-withdrawing −F and −CN substituents raise $E^{\circ\prime}$ more, 3.6 and 5.1 kcal/mol, respectively, for the **3** derivatives. There is a slightly larger effect for **3(CN)** than for **1(CN)**, although the difference is not very large. In keeping with this observation, the bicyclic frameworks present for these compounds have very little effect on how much replacing a hydrogen on a carbon β to a hydrazine nitrogen by cyano raises $E^{\circ\prime}$: $E^{\circ\prime}$($Me_2NNMe(CH_2CH_2CN)$) − $E^{\circ\prime}$($Me_2NNMe(CH_2CH_3)$) is 0.22 V,[6] the same as $E^{\circ\prime}$(**3(CN)**) − $E^{\circ\prime}$(**3**). The (gas phase) $\Delta\Delta H_f$ values calculated by AM1 for replacement of H by a substituent in **3(F)**, **1(CN)**, and **3(CN)** are 5.1, 6.6, and 6.9 kcal/mol, all somewhat larger than the observed $\Delta E^{\circ\prime}$ (kcal/mol) values (3.6, 4.2 and 5.1, respectively), so the effects on $E^{\circ\prime}$ are calculated qualitatively correctly by AM1. Because the experimental $E^{\circ\prime}$ values include solvation effects, it is difficult to assess how well AM1 calculations actually handle the effect of through-bond interaction between the hydrazine and substituent groups on ease of oxidation.

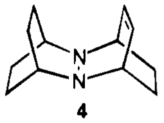

4

Geometries of 3 and 3^+. Thermal ellipsoid drawings of the X-ray structures of unsubstituted **3** and 3^+TsO^- are shown as Figures 4 and 5, respectively, and the geometries about the nitrogens are compared with those previously determined[7] for **1** and 1^+TsO^- in Table 3. **3** crystallizes in the same **1s2** invertomer as **3(OAc)**. The NN distance for **3** is essentially the same as that for **1** (most probable distance 0.008 Å longer, but estimated standard deviations are 0.003 and 0.004 Å). The N,N distance is known to increase as the lone pair, lone pair dihedral angle θ becomes closer to 0°, and θ values for **1** and **3** are 15.0 and 4.3°, respectively. The nitrogens are also more pyramidal in **3** than in **1**, presumably because of the smaller CNN angles forced in the 13 ring: α_{av} (the average of the bond angles at nitrogen) for **3** is 2.3° smaller than for **1**, which corresponds to 22% of the 10.5° change between a planar and a tetrahedral atom. An RHF/6-31G* geometry optimization of **3** got the NN bond length 0.034 Å shorter and α_{av} at nitrogen 1.4° larger than the X-ray structure.[8] The NN distance for 3^+TsO^-

---

[4] MM2 calculations get the *anti* lone pair conformation of **1** to be destabilized 9.9 kcal/mol relative to the *syn* conformation: Nelsen, S. F.; Wang, Y.; Powell, D. R.; Hiyashi, R. K. *J. Am. Chem. Soc.* **1993**, *115*, 5246.

[5] Conversely, if the less stable nitrogen inversion isomer of **2** were what is attacked, the calculated CN^+,N'lp twist angles χ are 148.3 and 84.3° for bond b and bond a respectively, $\cos^2\chi$ = 0.72 and 0.01, respectively, but bond b cleavage initially gives the unfavorable *anti* conformation of **3**. We can see no argument favoring the observed breakage of bond b if the less stable nitrogen inversion isomer of **2** is the substrate for S_N2 cleavage.

[6] Nelsen, S. F.; Parmelee, W. P.; Rumack, D. T. *J. Org. Chem.* **1983**, *48*, 4219.

[7] Nelsen, S. F.; Blackstock, S. C.; Haller, K. J. *Tetrahedron* **1986**, *42*, 6101.

[8] RHF/6-31G*-optimized geometry of **3**: d(NN) = 1.466 Å, ∠NNC(22) 111.0°, ∠NNC (31) 106.7°, ∠NCN 118.0°, α_{av} 111.9°. For comparison of *ab initio* and X-ray geometries for other hydrazines, see ref 4.

Table 3. Comparison of Geometry Changes at Nitrogen for Electron Removal from 1 and 3

	1	**3**
d(NN), Å	1.492(4)	1.500(3)
α(CNN), deg	108.7	105.4, 106.0 ($\underline{13}$ ring)
α(CNN), deg	111.0	110.2, 109.9 ($\overline{\underline{22}}$ ring)
α(CNC), deg	118.6	116.5, 115.1
α_{av}, deg	112.8	110.7, 110.3
θ, deg	15.0	4.3
	1$^+$TsO$^-$ [a]	**3**$^+$TsO$^-$
d(NN), Å	avg 1.332[b]	1.328(3)
α(CNN), deg	avg 114.0[c]	109.8, 110.1 ($\underline{13}$ ring)
α(CNN), deg		114.4, 114.9 ($\overline{\underline{22}}$ ring)
α(CNC), deg	avg 127.8[d]	133.1, 132.3
α_{av}, deg	avg 118.6[e]	119.1, 119.1
θ, deg	avg 4.0	0.7
	change	change
Δd(NN), Å	−0.160 (11.5%)	−0.172 (10.7%)
$\Delta\alpha_{av}$, deg	+5.8	+8.4

[a] From ref 5. Structure complicated by disorder in the anion as well as the presence of two independent cations, **a** and **b**, in the unit cell. [b] **a**: 1.339(14) Å. **b**: 1.325(13) Å. [c] **a**: 113.7(10), 113.1(8), 113.9(8), 114.1(9) Å. **b**: 114.2(9), 114.1(8), 114.1(8), 114.4(9) Å. [d] **a**: 130.3(10), 128.6(10) Å. **b**: 127.1(9), 124.8(9) Å. [e] **a**: 119.3, 118.6 Å. **b**: 118.5, 118.0 Å.

Table 4. Hyperfine Splitting Constant Data (G) for 1$^+$ and 3$^+$

species	type	NMR	ESR	ENDOR
1$^+$ [a,b]	N		15.1 (2N)	
	γ^{exo}	unobsd	2.87 (8H)	+2.80
	γ^{endo}	−0.60	0.59 (8H)	−0.56
	β^{br}	+0.09	unobsd	unobsd
3$^+$ [b,c]	N		15.34 (2N)	
	H		2.89 (4H)[d]	+2.87
	H		2.64 (4H)	+2.78
	H		0.65 (4H?)	−0.65
	H		0.51 (4H?)	−0.57

[a] From ref 4. [b] NMR at 300 K in CH_3CN, ESR at 297 K in CH_3CN, ENDOR at 240 K in toluene containing a trace of trifluoroacetic acid. [c] See text for discussion of assignments. [d] The 4_{ax}-d_1 ESR spectrum was well simulated using a(3H) = 2.89 G, a(1D) = 0.48 G, with the other parameters listed.

is close to that for **1**$^+$TsO$^-$. **3**$^+$TsO$^-$ has rather slight pyramidalization, α_{av} = 119.1° (only 8.6% of 10.5°), but it is in the **3s2** invertomer, the alternate one to that of the neutral compound. We believe that the tosylate placement in the crystal determines the sense of pyramidalization, because with such small amounts of pyramidalization, the two invertomers should have nearly the same energy. The closest tosylate oxygen to nitrogen distance is 3.269 Å, and the NNO angle 151.1°, and neither the distance nor the position relative to the NN π system is in the range found to affect the NN distance for trialkyldiazenium cations.[9] It seems surprising that **3**$^+$ is flatter at nitrogen than is **1**$^+$ or other sesquibicyclic hydrazine radical cations, because the neutral compounds are in the expected order for pyramidality, **3** more pyramidal than **1**. The difference in α_{av} for **1**$^+$ and **3**$^+$ is, however, rather small, 0.5°. The change in α_{av} upon electron loss is significantly larger for **3** than for **1**, 80% of 10.5° versus 55%.

Hyperfine splitting constants provide a way of studying the solution conformations of radicals. ENDOR, ESR, and NMR studies of **1**$^+$ have shown that γ^{exo}(8H), γ^{endo}(8H), and β^{br}(4H) splittings are present,[10] so double nitrogen inversion is fast on the ESR time scale, as expected from AM1 calculations of the barrier to double nitrogen inversion. Hyperfine splitting constant data for **1**$^+$ and **3**$^+$ are summarized in Table 4. The nitrogen splitting constant is slightly larger for **3**$^+$, but although a(N) increases as pyramidality increases, it also probably increases as the CNN angle decreases, and we do not believe that any conclusion can be drawn about how flat the nitrogens are in solution from these two numbers. Both ESR and ENDOR spectra for **3**$^+$ are consistent with two a(4H) splittings, 2.87–2.89 and 2.64–2.78 G, which requires that two pairs of splittings are unresolved. The γ-hydrogens in W-plan with the spin-bearing p-rich orbitals at nitrogen will show large splittings, as demonstrated by the splittings observed by Russell and coworkers for the $\underline{22}$ semidione **5** (a(4H-γ^{exo}) = 2.09 G)[11a] and the $\underline{31}$ semidione **6** (a(2H-γ^{ax}) = 5.51 G).[11b] The ESR spectrum of the (**3**-4^{ax}-d_1)$^+$ sample was well simulated using a(3H) = 2.89 G, a(1D) = 0.48 G, and the other splittings from Table 4, showing that the $\underline{31}$ ring γ^{ax} pair of hydrogens contributes to the largest observed hydrogen splitting. Previous studies of hydrazines containing $\underline{22}$ rings have shown that the γ splittings are very sensitive to nitrogen pyramidalization and are only large for W-plan splittings.[10] Despite the small amount of pyramidalization at nitrogen present for **3**$^+$, very different splittings are expected for the two invertomers, which should be equilibrating rapidly on the ESR time scale,[12] so that the observed splittings are weighted averages of those for the two invertomers. The fourth large splitting for **3**$^+$ is assigned to the $\underline{31}$ ring bridgehead hydrogens. The singly occupied molecular orbital of semidiones is symmetrical through a plane bisecting the CC bond between the carbonyl oxygens, while that of hydrazine radical cations is antisymmetrical through the plane bisecting the NN bond, making **6** a very poor model for the splittings of hydrogens of **3**$^+$ which interact with both nitrogens.[11c] This obviously includes the $\underline{31}$ ring bridgehead hydrogens, which we pointed out previously must have important spin contribution from the γ nitrogen.[10] According to predictions based upon AM1 calculations[13] which are summarized in Figure 6, the **3s2** invertomer will show large splittings for the W-plan γ^{exo} at the $\underline{2}$ bridge *syn* to the $\underline{1}$ bridge and γ^{ax} in the $\underline{13}$ bridge and

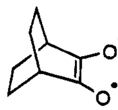
5

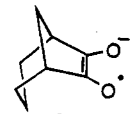
6

---

(9) Nelsen, S. F.; Chang, H.; Wolff, J. J.; Powell, D. R. *J. Org. Chem.* **1994**, *58*, 6558.

(10) Nelsen, S. F.; Petillo P. A.; De Felippis, J.; Wang, Y.; Chen, L.-J.; Yunta, M. J. R.; Neugebauer, F. A. *J. Am. Chem. Soc.* **1993**, *115*, 5608.

(11) (a) Russell, G. A.; Chang, K. Y. *J. Am. Chem. Soc.* **1965**, *87*, 4381. (b) Russell, G. A.; Chang, K. Y.; Jefford, C. W. *Ibid.* **1965**, *87*, 4383. (c) **6** shows a single hydrogen splitting of 4.03 G assigned as 8-anti and five 0.53 G splittings, to which the bridgehead splittings were assigned.[11b]

(12) Nelsen, S. F.; Frigo, T. B.; Kim, Y. Blackstock, S. C. *J. Am. Chem. Soc.* **1989**, *111*, 5387.

(13) The splittings shown in Figure 6 were calculated using an unpublished method developed by Timothy Clark and S.F.N. which is based on a neural net which uses as input the hydrogen spin density calculated by three methods, the UHF charge density, and the total molecular charge and was "trained" using literature data. Most of the information on γ splittings in the training set comes from 2,3-dioxabicyclo[2.2.2]octane radical cation. It is far better for long-range splittings than previous methods. The bridgehead β-splitting is unlikely to be very accurate because of a lack of suitable training data. The method used has not been published because we are presently working on a better neural-net-based procedure.

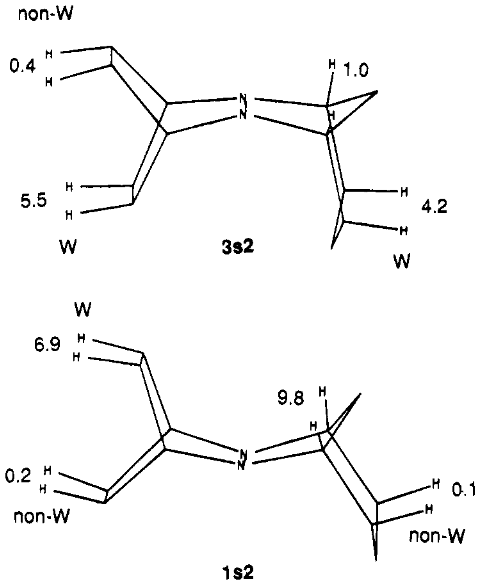

Figure 6. Stick drawings of the AM1 structures of the **3s2** and **1s2** invertomers of $\mathbf{3}^+$, showing only the hydrogens expected to show splittings >2 G in the equilibrating mixture. The numbers written next to the hydrogens are splitting constants in Gauss estimated from AM1 calculations at the energy minima.[13]

the **1s2** invertomer will show large splittings for the W-plan γ^{exo} at the 2 bridge *syn* to the 3 bridge and for β^{br} of the 13 bridge. All of the other hydrogens of $\mathbf{3}^+$ are calculated to have small splittings in both invertomers. Because the calculated splittings are very sensitive to nitrogen pyramidality and AM1 probably gets the nitrogens too pyramidal at least for the **3s2** invertomer (for which AM1 gets 118.1°, while the x-ray structure has 119.1°; AM1 gets 117.4° for the **1s2** invertomer, and of course the positions of the energy minima might well be different in solution than they are in a crystal), and because of inaccuracies in the calculation method used, we do not believe that we can accurately predict the averaged splittings from the calculated AM1 energy surface. The conclusion that there are four pairs of splittings which will be above 2 G if and only if **1s2** and **3s2** are about equally occupied appears firm, and we assign the two observed 2.6–2.9 G splittings to the four pairs of hydrogens shown in Figure 6. As pointed out previously,[10] the γ^{exo} splittings for 22 sesquibicyclic hydrazines with an unsymmetrical second ring are extremely sensitive to the mole fractions of the two invertomers. Use of eqs 4–7 of ref 10 with the observed ENDOR splittings and the 5.5–6.25 range for A_W in 22 systems previously discussed produces the mole fraction of the major invertomer in the narrow range of 0.506–0.508, corresponding to $\Delta G°$ under 0.02 kcal/mol. The tiny energy difference between the **1s2** and **3s2** invertomers of $\mathbf{3}^+$ obtained from the hyperfine splittings in solution is quite consistent with the almost planar nitrogens found in the X-ray crystal structure, making it seem unlikely to us that the flattening relative to $\mathbf{1}^+$ found in the X-ray structure is an artifact of crystal packing forces. $\mathbf{3}^+$ unfortunately reacts too rapidly with di-*tert*-butyl nitroxide to allow a detailed NMR study,[10] which would probably have been able to resolve the small splittings. Signals corresponding to two small negative splittings were observed in the ENDOR spectrum and are of the size expected for the 22 ring γ^{endo} signals,[10] but ESR spectral simulations indicate that two or four 13 ring hydrogen splittings are also of similar magnitude.

Comparison of Electron Transfer Rate Constants for 1 and 3. **1** and **3** are so similar in size and structure that self-electron transfer rate constants k_{ex} for exchange between the neutral compound and its own radical cation should principally reflect changes in the Marcus inner sphere geometry reorganization parameter, λ_{in}. Hydrazines have unusually large λ_{in} values because of their large geometry change upon electron removal, which is the principal cause of their small k_{ex} values compared to other organic compounds.[14] The more difficult oxidation of **3** than **1** is not a direct factor in determining k_{ex}, which is for a thermoneutral process in both cases. The largest k_{ex} known for a hydrazine is for the even more CNN angle-restricted and difficult to oxidize 21/21 compound **7**, $k_{ex}(25\ °C) = 1.85 \times 10^4$, while that for $\mathbf{1}^{0/+}$ is about 700 $M^{-1}\ s^{-1}$.[14] The significant twist about the NN bond of **1** rather clearly makes its k_{ex} values smaller than those of untwisted hydrazines of the same ring size. Twisting at the NN bond raises the relaxation enthalpy of the radical cation significantly, which should increase λ_{in}. The unsaturated analogue of **1**, **4** (22/u22),[15] has similar experimental $\Delta d(NN)$ and $\Delta\alpha_{av}$ values to those of **1** because the bicyclic rings are of the same size, but has much less twisting in the neutral form because of the double bond (see Table 5). $\mathbf{4}^{0/+}$ has a 17-fold faster k_{ex}(25 °C) than does $\mathbf{1}^{0/+}$, corresponding to a 1.7 kcal/mol smaller $\Delta G^{\ddagger}$ (and four times this change in λ_{in}, if λ_{in} change is the only factor affecting $\Delta G^{\ddagger}$), indicating that NN bond twisting is indeed a significant factor in making k_{ex} for $\mathbf{1}^{0/+}$ small. Because AM1 calculations of λ'_{in}, the enthalpy contribution to λ_{in}, carried out as described previously,[16] gave a linear plot with the observed changes in $\Delta G^{\ddagger}_{ex}$ for **7**, **4**, and three other untwisted analogues (23/u23, 22/u23, and 21/u22),[14] we had expected that **3** would show k_{ex} smaller than **4**, but probably near the ~3000 $M^{-1}\ s^{-1}$ predicted by AM1 calculation of λ'_{in} for **3**. This does not prove to be the case. Very little line broadening is observed upon mixing $\mathbf{3}^+$ with **3**, and k_{ex}(25 °C) for $\mathbf{3}^{0/+}$ is estimated to be about 300 $M^{-1}\ s^{-1}$ (see the Experimental Section for the data and Table 5 for comparison of experimental results with AM1 calculations for **4**, **1**, **3**, and **7**), although with so little broadening being observed, this number cannot be considered very accurate. We suspect that the too small geometry changes obtained by AM1 for electron removal from **3** are at least partially responsible for the failure of AM1 calculations to predict a large enough barrier for the self-ET of $\mathbf{3}^{0/+}$ and note that the predictive power of AM1 calculations for the k_{ex} difference between $\mathbf{1}^{0/+}$ and $\mathbf{3}^{0/+}$ is clearly poor. We conclude that the combination of larger $\Delta\alpha_{av}$ and $\Delta d(NN)$ for $\mathbf{3}^{0/+}$ outweighs the effect of its smaller $\Delta\theta$ value and that λ_{in} is probably slightly larger for $\mathbf{3}^{0/+}$ than for $\mathbf{1}^{0/+}$, although it must be admitted that we do not know how to estimate possible differences in electronic transmission coefficient, κ_{el} for these closely related compounds.

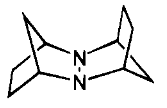

7

---

[14] Nelsen, S. F.; Wang, Y. *J. Org. Chem.* **1994**, *59*, 1655.

[15] (a) Nelsen, S. F.; Blackstock, S. C. *J. Am. Chem. Soc.* **1985**, *107*, 7189. (b) Nelsen, S. F.; Kim, Y.; Blackstock, S. C. *J. Am. Chem. Soc.* **1989**, *111*, 2045.

[16] Nelsen, S. F.; Blackstock, S. C.; Kim, Y. *J. Am. Chem. Soc.* **1987**, *109*, 677.

Table 5. Comparison of Experimental k_{ex} Values and Geometry Changes with AM1-Calculated Geometries and Relaxation Enthalpies (kcal/mol) for Hydrazine Self-Exchanges

	4 ($\underline{22/u22}$)	**1** ($\underline{22/22}$)	**3** ($\underline{22/13}$)	**7** ($\underline{21/21}$)
Exchange Rates (by NMR Line Broadening)				
k_{ex}, $M^{-1}\ s^{-1}$	12 100 ± 1000	~700	~300	18 500 ± 500
$\Delta G^{\ddagger}{}_{ex}{}^{a}$	11.89(5)	~13.6	~14.1	11.63(5)
$\Delta\Delta G^{\ddagger}{}_{ex}{}^{a}$	[≡0]	~+1.7	~+2.2	−0.26
Geometry Changes upon Electron Loss				
	X-ray (AM1)	X-ray (AM1)	X-ray (AM1)	(AM1)
$\Delta\theta$, deg	0.4 (0.0)	11.0 (0.0)	3.6 (0.0)	(0.0)
Δd(NN), Å	−0.148 (−0.086)	−0.160 (−0.084)	−0.172 (−0.092)	(−0.078)
$\Delta\alpha_{av}$, deg	+5.6 (+5.7)	+5.8 (+4.6)	+8.4 (+6.6)	(5.9)
AM1-Calculated Inner Sphere Reorganization Energies				
$\Delta H_r(\mathbf{c})^a$	15.64	15.36	16.82	15.78
$\Delta H_r(\mathbf{n})^a$	20.93	17.84	22.71	19.47
$\lambda'_{in}{}^{a}$	36.57	33.20	39.53	35.25
$\Delta\lambda'_{in}/4^a$	[≡0]	−0.84	+0.74	−0.33

[a] Unit: kcal/mol.

Conclusions

Cleavage of **2** by nucleophiles gives mostly **3(X)**: we could not even reliably detect **1(OAc)** or **1(F)**, although the softer nucleophiles PhS^- and CN^- gave 40 and 15% **1(X)**, respectively. The change in substitution pattern in going from **1** to **3** causes a large change in standard potential for electron removal (8.4 kcal/mol), and replacement of a γ-hydrogen by an electron-withdrawing substituent raises $E^{\circ\prime}$ detectably. Although the neutral 1,3-dinitrogen bridged cyclohexane derivative **3** has more pyramidal nitrogens than does its 1,4-bridged analogue **1**, its radical cation $\mathbf{3}^+$ has more planar nitrogens than does $\mathbf{1}^+$. This turn-around in pyramidality is not predicted by AM1 calculations, and we do not know why it occurs. The self-ET k_{ex}(25 °C) for $\mathbf{3}^{0/+}$ is about 300 $M^{-1}\ s^{-1}$, indicating that the increase in change of nitrogen pyramidality and NN bond length outweighs the smaller change in NN twist angle for $\mathbf{3}^{0/+}$ relative to $\mathbf{1}^{0/+}$.

Experimental Section

Solvents. Acetonitrile was distilled from CaH_2, diethyl ether was distilled from purple sodium benzophenone ketyl under a N_2 atmosphere, and pentane was stirred with sulfuric acid, washed with water, saturated sodium bicarbonate solution, and water, dried over magnesium sulfate and molecular sieves, and distilled over CaH_2. Pyridine was distilled over CaH_2 and stored over molecular sieves. Deuterated solvents were stored over molecular sieves.

2,8-Diazatetracyclo[7.2.2.1^{3,7}.0^{2,8}]tetradecane, 3.[2] A solution of 1.1346 g (2.353 mmol) of dication $\mathbf{1}^{2+}(PF_6^-)_2$ in 50 mL of anhydrous acetonitrile was purged with Ar at −25 °C. Into this solution was added *via cannula* 360 μL (4.45 mmol) of anhydrous pyridine, and after being kept at −25 °C for 21 h the solution was transfered *via cannula* to a 100 mL flask containing 550.1 mg (5.87 mmol, 2.50 equiv) of tetramethylammonium borohydride (95% pure) in 5 mL of anhydrous acetonitrile. The mixture was magnetically stirred under Ar at −25 °C for 17 h and then extracted with pentane. Upon removal of pentane under reduced pressure, 451.3 mg (99.7%) of a solid was obtained which ^1H NMR indicated was a mixture of **1** and **3** in 0.8:1.0 molar ratio. This mixture was dissolved in 10 mL of anhydrous acetonitrile and cooled to 0 °C, and a solution of 180.2 mg (0.989 mmol) of $NOPF_6$ (96% pure) in 5.0 mL of acetonitrile was added *via cannula*. After the mixture was stirred at 0 °C for 1 h and extracted with pentane, concentration under reduced pressure gave 201.3 mg of a slightly orange solid. Sublimation of the solid at 36 °C (0.9 mmHg) gave 113.9 mg of **3** (44.6%), mp 54−55 °C. Empirical formula $C_{12}H_{20}N_2$ established by HRMS: calcd 192.1626, obsd 192.1640. The structure of **3** was verified by X-ray crystallography. ^1H-NMR ($CDCl_3$) δ: 3.40 (2H, ~t, *J* = 5.5 Hz, **3b,7b**); 2.77 (2H, br s, **1b, 9b**); 2.13−2.22 (3H, br, **12n, 13n, 14s**); 1.91 (2H, complex, **10n, 11n**); 1.82 (1H, pattern ~*3J*; *2J*/*2*, **5ax**); 1.6−1.7 (4H, complex, **12x, 13x, 4eq, 6eq**); 1.48 (1H, pattern ~*J*; *2J*/*2*, **5eq**); 1.39−1.43 (3H, complex, **10x, 11x, 14a**); 1.29 (2H, pattern ~*2J*; *J*/*2*, **4ax, 6ax**). ^{13}C-NMR ($CDCl_3$) δ: 61.09 (C_3, C_7); 51.38 (C_1, C_9); 37.59 (C_{14}); 33.87 (C_4, C_6); 28.24 (C_{12}, C_{13}); 21.13 (C_{10}, C_{11}); 18.05 (C_5). The $\underline{22}$ ring signals were assigned by analogy with those of $\underline{22/21}$, previously assigned with the aid of deuteration and H,H-COSY.[9]

4-ax-Deuterio-2,8-diazatetracyclo[7.2.2.1^{3,7}.0^{2,8}]-tetradecane, 3-*d*$_1$. A solution of 624.2 mg (1.294 mmol) of dication $\mathbf{1}^{2+}(PF_6^-)_2$ in 35 mL of anhydrous acetonitrile at −25 °C under N_2 was treated with 1 mL of anhydrous pyridine and, after 2 h at −25 °C under N_2, was added *via cannula* to 107.2 mg (2.304 mmol, 1.78 equiv) of 98-D% sodium borodeuteride (90% pure) at −25 °C. The mixture was stirred at −25 °C under N_2 for 18 h, extracted with pentane, and concentrated to give 239.3 mg (95.7%) of a solid which ^1H NMR showed was a mixture of **3**-d_1 and **1**-d_1 in 1:0.2 mol ratio. This mixture in 15 mL of anhydrous acetonitrile was added *via cannula* to 24.5 mg (0.144 mmol) of $AgNO_3$, and the mixture was stirred for 1 h. After extraction with pentane and concentration 136.3 mg of a white solid was obtained, which was sublimed at 45 °C, 0.2 mmHg, giving 74 mg of **3**-d_1, mp 56−59 °C. This material was unfortunately contaminated with a detectable amount of **1**-d_1, as shown by NMR. ^2H-NMR ($CDCl_3$) δ: 1.275, peak for **1**-d_1 detected at δ 1.63. ^{13}C-NMR ($CDCl_3$) δ: 61.08, 61.01 (C_3, C_7); 51.38; 37.57; 33.88 (C_6); 33.49 (t, J_{CD} = 17.9 Hz); 28.25; 21.13; 18.86 (peaks for **1**-d_1 also detected at 50.91, 27.28, 27.20).

4-*ax*-(Phenylthio)-2,8-diazatetracyclo[7.2.2.1^{3,7}.0^{2,8}]-tetradecane, 3(SPh) and 4-*exo*-(Phenylthio)-2,8-diazatetracyclo[6.2.2.2^{3,6}.0^{2,7}]tetradecane, 1(SPh). A solution of 747.6 mg (1.55 mmol) of dication $\mathbf{1}^{2+}(PF_6^-)_2$ in 40 mL of anhydrous acetonitrile at −25 °C was treated with 2 mL of pyridine under N_2, kept at −25 °C for 6 h, and added *via cannula* to 263.8 mg (1.99 mmol, 1.29 equiv) of sodium thiophenoxide. The mixture was stirred at −25 °C under N_2 for 17 h and then extracted with pentane and concentrated under reduced pressure to give 443.8 mg of a solid which by ^1H NMR was principally a mixture of **1(SPh)** and **3(SPh)** in 1.0:1.5 ratio (95.3%). Fractional recrystallization of the product mixture from pentane−ether (1:1) and acetonitrile gave both **1(SPh)** and **3(SPh)** in pure forms. The structure of **1(SPh)**, mp 103−104 °C, was verified by X-ray crystallography. Empirical formula $C_{18}H_{24}N_2S$ established by HRMS: calcd 300.1660, obsd 300.1668. Anal. Calcd: C, 71.95; H, 8.505; N, 9.32. Found: C, 72.25; H, 8.50; N, 9.26. ^1H NMR ($CDCl_3$) δ: 7.30−7.34 (m, 2H); 7.17−7.23 (m, 2H); 7.09−7.14 (m, 1H); 4.05−4.15 (m, 1H); 2.62−2.77 (m, 5H); 2.35−2.45 (m, 1H); 2.05−2.36 (m, 7H); 1.52−1.70 (m, 5H); 1.50−1.46 (ddd, *J* = 13.5, 5.5, 1.5, 1H). ^{13}C NMR ($CDCl_3$) δ: 135.82; 130.52; 128.89; 126.38; 54.07; 51.72; 50.98; 50.87; 44.84; 36.81; 28.37; 28.10; 26.43; 26.24; 25.94; 20.49. **3(SPh)**: mp 95−96 °C. Empirical formula $C_{18}H_{24}N_2S$ established by HRMS: calcd 300.1660, obsd 300.1671. ^1H NMR ($CDCl_3$) δ: 7.35 (2H, ~dm o); 7.24 (2H, ~tm, m); 7.16 (1H, ~tt, p); 3.50 (1H, ~t, *J* = 5.2, **3b**); 3.49 (1H, br, **7b**); 3.43 (1H, m, **4eq**); 2.80 (1H, br s, **1b**); 2.70 (1H br s, **9b**); 2.22−2.37 (1H, m, **5ax**); 2.11−2.16 (2H, m, **12n, 13n**);

2.08 (1H, ~d, J = 12.0, **14s**); 1.96–2.01 (1H, complex, **5eq**); 1.80–1.94 (2H, m, **10n**, **11n**); 1.62–1.68 (2H, br d, **12x**, **13x**?); 1.54–1.62 (3H, complex, **10x**, **11x**?, **14a**); 1.35–1.46 (2H, m, **6eq**, **6ax**). ^{13}C NMR (CDCl$_3$) δ: 135.98, 130.52, 128.89, 126.25; 64.77 (C_3); 61.01 (C_7); 51.43 (C_1, C_9); 49.54; 32.35; 30.51; 28.08; 24.70; 21.10 (C_{10}, C_{11}).

4-*ax*-Cyano-2,8-diazatetracyclo[7.2.2.1^{3,7}.0^{2,8}]tetradecane, 3(CN). A solution of 363.4 mg (0.754 mmol) of dication $\mathbf{1}^{2+}(PF_6^-)_2$ in 40 mL of anhydrous acetonitrile was purged with Ar at −25 °C, and 0.80 mL (9.86 mmol, 13 equiv) of anhydrous pyridine was injected. The solution was stored at −25 °C under argon for 90 min and then added *via cannula* to a 100ml round bottom flask containing 359.3 mg (1.285 mmol, 1.70 equiv) of tetrabutylammonium cyanide (96% pure) at −25 °C. The mixture was stirred at −25 °C under N_2 for 17 h. During the course of the reaction the solution turned bright orange in color. Extraction of the solution with pentane and removal of solvent under reduced pressure gave 163.8 mg (102%) of a solid which ^{1}H NMR indicated consisted of about 80% **3(CN)** and minor amounts of **1** and **1(CN)**. Recrystallization from ether removed **1**, giving 112.8 mg of material which was a 0.14_5:0.85_5 mixture of **1(CN)**:**3(CN)** by ^{1}H-NMR (68.8% yield of the mixture based on $\mathbf{1}^{2+}$). A 73.3 mg (0.361 mmol) aliquot of this mixture in 10 mL of anhydrous acetonitrile was treated with 8.9 mg (0.052 mmol) of $AgNO_3$, and the mixture was stirred under N_2 for 5 min and extracted with pentane. Upon removal of pentane under reduced pressure, a hygroscopic solid was obtained which was crystallized from ether at −25 °C to give 53.3 mg of **3(CN)** (50% based on $\mathbf{1}^{2+}$), mp 104–106 °C. Empirical formula $C_{13}H_{19}N_3$ established by HRMS: calcd 217.1579, obsd 217.1575. ^{1}H NMR (CDCl$_3$) δ: 3.55 (1H, ~t, **3b**); 3.40 (br t, J ~ 4.5 Hz, **7b**); 2.75–2.77 (3H, complex, **1b**, **9b**, **4eq**); 2.05–2.15 (4H, m, **12n**, **13n**, **14a**, **5ax**); 1.90 (1H, ~d, J = 12.5 Hz, **14s**); 1.80–1.92 (2H, complex, **10n**, **11n**); 1.65 (dd J = 13.5, 4.5 Hz, **5eq**); 1.55–1.65 (3H, complex, **6ax**, **12x**, **13x**); 1.42–1.50 (1H, tdd, J = 13.0, 4.5, 1.5 Hz, **6eq**); 1.35–1.45 (2H, ~br d, **10x**, **11x**). ^{13}C NMR (CDCl$_3$) δ: 121.67 ($C{\equiv}N$); 67.95 (C_3); 66.06 (C_7); 57.08, 57.04 (C_1, C_9); 39.56 (C_{14}); 39.30 (C_4); 37.00 (C_6); 33.83, 33.70 (C_{12}, C_{13}); 28.42, 26.87 (C_{10}, C_{11}); 26.67 (C_5). Assignments employed C, H correlations established by heteronuclear multiple quantum coherence experiments.[17]

4-*ax*-Acetoxy-2,8-diazatetracyclo[7.2.2.1^{3,7}.0^{2,8}]-tetradecane, 3(OAc). A solution of 287.6 mg (0.596 mmol) of dication $\mathbf{1}^{2+}(PF_6^-)_2$ in 25 mL of anhydrous acetonitrile was treated with 70 μL (0.865 mmol) of pyridine at −25 °C under argon and, after 3.5 h, was added *via cannula* to a solution of 749.0 mg (2.837 mmol) of tetraethylammonium acetate tetrahydrate (99% pure) in 10 mL of anhydrous acetonitrile at −25 °C. The mixture was stirred at −10 °C for 14 h and then at 0 °C for 1 h and extracted with pentane. Removal of pentane under reduced pressure gave 141.7 mg of a solid which ^{1}H NMR indicated was a 1.0:0.2 mixture of **3(OAc)** and **1**, corresponding to 98.9% yield of these products based on $\mathbf{1}^{2+}$. This material was dissolved in 10 mL of anhydrous acetonitrile, 17.5 mg (0.096 mmol) of $NOPF_6$ (96%) in 1 mL of anhydrous acetonitrile was added *via cannula*, and after being stirred for 5 min the solution was extracted with 6 × 15 mL portions of pentane. Removal of solvent under reduced pressure and sublimation at 50–55 °C (0.1 mmHg) gave 60.4 mg (40.5%) **3(OAc)**, mp 118–119 °C. Empirical formula $C_{14}H_{22}N_2O_2$ established by HRMS: calcd 250.1681, obsd 250.1687. Anal. Calcd C, 67.17; H, 8.86; N, 11.19. Found: C, 67.02; H, 8.85; N, 11.17. The structure of **3(OAc)** was verified by X-ray crystallography. ^{1}H NMR (CDCl$_3$) δ: 4.74 (1H, m, **4eq**); 3.59 (1H, ~t, J = 5.2 Hz, **3b**); 3.37 (1H, ~t, J = 5.1, **7b**); 2.79, 2.76 (1H, br s; 1H, br s, **1b**, **9b**); 2.0–2.15 (6H, complex); 2.03 (3H, s) **Me**; 1.80–1.95 (4H, complex); 1.6–1.7 (2H, br d, J = 8.1 Hz); 1.5–1.6 (1H, m); 1.35–1.5 (4H, complex). ^{13}C-NMR (CDCl$_3$) δ: 170.54 ($C{=}O$); 73.22 (C_4); 62.65 (C_3); 60.53 (C_7); 51.30, 51.27 (C_1, C_9); 31.18 (C_{14}); 30.63 (C_6); 28.14, 27.99 (C_{12}, C_{13}); 24.07 (C_5); 21.49 (CH_3); 21.21, 21.05 (C_{10}, C_{11}).

4-*ax*-Fluoro-2,8-diazatetracyclo[7.2.2.1^{3,7}.0^{2,8}]tetradecane, 3(F). A solution of 367.5 mg (0.762 mmol) of $\mathbf{1}^{2+}(PF_6^-)_2$ in 20 mL of anhydrous acetonitrile at −25 °C was injected with 130 μL (1.77 mmol) of pyridine, kept at −25 °C for 19 h, and then added *via cannula* to 631.1 mg of $BnMe_3NF{\cdot}xH_2O$ (97%) and 5 mL of acetonitrile. The mixture was stirred under N_2 at −25 °C for 20 h, extracted with pentane, and concentrated to give 85.5 mg (53%) of material which ^{1}H NMR showed was a mixture of **1(F)**:**3(F)** in a 0.65:1.00 molar ratio. A solution of this material in 4 mL of acetonitrile was added via cannula to 36.8 mg (0.202 mmol) of $NOPF_6$, and the mixture was stirred under N_2 for 10 min, extracted with pentane, and concentrated to give 65.3 mg (40.8%) of **3(F)**, mp 82–83 °C. Empirical formula $C_{12}H_{19}N_2F$ established by HRMS: calcd 210.1532, obsd 210.1554. ^{1}H NMR (CDCl$_3$) δ: 4.65 (1H, dt, J = 51.1, 4.1 Hz, **4eq**); 3.57 (1H, ~t, J = 5.0 Hz, **3b**); 3.35 (1H, br t, **7b**); 2.79 (1H, br, **1b**); 2.78 (1H, br, **9b**); 2.08–2.16 (2H, complex); 1.87–2.08 (6H, complex); 1.59–1.71 (4H, complex); 1.40–1.58 (2H, complex). ^{13}C NMR (CDCl$_3$) δ 90.60 (C_4, $^{1}J_{CF}$ = 173 Hz); 63.50 (C_3, $^{2}J_{CF}$ = 25 Hz); 60.30 (C_7); 51.44, 51.22 (C_1, C_9); 30.70 (C_6, $^{3}J_{CF}$ = 2.8 Hz); 30.40 (C_{14}); 28.09, 27.97 (C_{12}, C_{13}); 24.72 (C_5, $^{2}J_{CF}$ = 20 Hz); 22.13, 21.09 (C_{10}, C_{11}).

$\mathbf{3}^{\cdot+}$ OTs$^-$. A solution of 37.2 mg (0.193 mmol) of **3** in 2 mL of dichloromethane was cooled to −78 °C under Ar and added *via cannula* to 54.1 mg (0.193 mmol, 1.0 equiv) of silver *p*-toluenesulfonate at −25 °C. The mixture was stirred at −78 °C for 1 h, filtered to remove Ag solid, and concentrated under reduced pressure to give a white solid which was recrystallized in acetonitrile by diffusion of ether vapor at −25 °C, dec 162–164 °C. The structure was verified by X-ray crystallography.

$\mathbf{3}^{\cdot+}$ NO$_3^-$. A solution of 107.0 mg (0.556 mmol) of **3** in 25 mL of anhydrous dichloromethane was purged with Ar and added *via cannula* to 97.9 mg (0.576 mmol) of $AgNO_3$ cooled to −78 °C. The mixture was stirred at −78 °C under Ar for 0.5 h, silver was filtered off, and solvent was removed under reduced pressure. The residue was recrystallized in acetonitrile by diffusion of ether vapor at −25 °C, dec 220–224 °C. Anal. Calcd for $C_{12}H_{20}N_3O_3$: C, 56.68; H, 7.93; N, 16.52. Found: C, 56.44; H, 7.83; N, 16.46.

$\mathbf{3}^{0/\cdot+}$ Electron Exchange Line Broadening. A solution of 11.17 mg (0.058 mmol) of **3** in 500 μL of MeCN-d_3 (0.116 M) in an NMR tube was deaerated with Ar, and the spectrum at 20.6 °C was recorded after 0, 15, 30, 30, 25, 50, 50, and 50 μL aliquots of a solution of 3.3 mg (0.013 mmol) of $\mathbf{3}^+NO_3^-$ in 300 μL of MeCN-d_3 were added. Only tiny line broadenings were observed, but the sharp lines of **3** make line broadening unusually easy to determine. Line broadening, Hz [[$\mathbf{3}^+$], mM] pairs: 0.15 [1.25], 0.21 [3.57], 0.35 [5.64], 0.40 [7.21], 0.55 [9.98], 0.70 [12.36], 0.90 [14.41]. This corresponds to k_{ex} of about 180 $M^{-1}\,s^{-1}$, although accuracy is limited by the small amount of broadening observed. Two variable temperature runs at constant concentration were carried out. Run 1: [**3**] = 137.1 mM, [$\mathbf{3}^+NO_3^-$] = 7.86 mM, T, °C [line broadening, Hz] pairs, 20.8 [0.8], 25.2 [0.85], 30.4 [0.9], 35.5 [1.0], 40.5 [1.1], 45.4 [1.2], 50.5 [1.3], produces interpolated k_{ex}(25 °C) of 340 $M^{-1}\,s^{-1}$. Run 2: [**3**] = 139.2 mM, [$\mathbf{3}^+NO_3^-$] = 7.15 mM, T, °C [line broadening,Hz] pairs, 20.5 [0.65], 25.3 [0.70], 30.3 [0.71], 40.3 [0.8], 45.3 [0.85], 50.3 [0.97], produces interpolated k_{ex}(25 °C) of 300 $M^{-1}\,s^{-1}$.

Crystal Structures. For a summary of crystal data and refinement parameters see Table 6. Data were collected on a Siemens P4 diffractometer using Cu Kα radiation (λ = 1.541 78 Å). The structure of **3(OAc)** was solved using SHELXTL PLUS (SGI)[18a] by direct methods and used full-matrix least-squares refinement of $\Sigma w(F_o - F_c)^2$ using SHELXL programs. Hydrogen atoms were located in a difference map and used the riding model with isotropic U and weighting scheme $w^{-1} = \sigma^2(F) + 0.0010F^2$. The structures of **3**, $\mathbf{3}^+(\mathbf{TsO}^-)$, and **1(SPh)** were solved using SHELXS-86[18b] and refined using full-matrix least-squares refinement on F^2 using SHELXL programs.[18c] Hydrogen atoms were located in a difference map

---

[17] Müller, L. *J. Am. Chem. Soc.* **1979**, *101*, 4481.

[18] (a) Sheldrick, G. M. (1990) SHELXTL PLUS, Version 4.2, Siemens Analytical X-ray Instruments, Inc., Madison, WI. (b) Sheldrick, G. M. SHELXS86. In *Crystallographic Computing 3*; Sheldrick, G. M., Krüger, C., Goddard, R., Eds.; 1985; pp 175–189. Sheldrick, G. M. *Acta Crystallogr.* **1990**, *A46*, 467–473. (c) Sheldrick, G. M. *J. Appl. Crystallogr.* Manuscript in preparation.

Table 6. Summary of Crystal Data and Refinement Parameters

compd no.	3	$3^{+}TsO^{-}$	3(OAc)	1(SPh)
empir form.	$C_{12}H_{20}N_2$	$C_{19}H_{27}N_2O_3S$	$C_{14}H_{22}N_2O_2$	$C_{18}H_{24}N_2S$
temp (K)	173(2)	113(2)	113(2)	113(2)
cryst size (mm)	0.5 × 0.4 × 0.1	0.4× × 0.4 × 0.2	0.5 × 0.4 × 0.3	0.4 × 0.2 × 0.05
cryst syst	triclinic	triclinic	monoclinic	triclinic
space grp	$P\bar{1}$	$P\bar{1}$	$P2_1/n$	$P\bar{1}$
a, Å	6.0795(4)	9.3769(8)	9.8813(8)	6.342(2)
b, Å	8.1593(5)	10.0046(11)	9.8842(9)	10.345(4)
c, Å	11.2424(9)	11.0560(6)	13.3742(13)	11.650(4)
α, deg	74.221(4)	65.817(6)		92.52(2)
β, deg	88.287(7)	81.107(6)	106.531(8)	96.76(2)
γ, deg	74.088(6)	68.320(8)		96.84(2)
volume, Å^3	515.50(6)	879.23(13)	1252.2(2)	752.3(5)
Z	2	2	4	2
density (calcd), mg/m^3	1.239	1.373	1.328	1.326
F(000)	212	390	544	324
index ranges	$-1 \le h \le 10, -1 \le k \le 9, -13 \le 1 \le 13$	$0 \le h \le 10, -9 \le k \le 9, -12 \le 1 \le 12$ + Friedel	$-1 \le h \le 10, -1 \le k \le 10, -14 \le 1 \le 14$	$0 \le h \le 6, -11 \le k \le 11, -12 \le 1 \le 12$
ω range, deg	1.88–25.00	4.38–56.98	3.00–40.00	1.50–22.50
reflcns collected	1587	4463	2289	3396
indept reflcns	1472 (0.0215)	2288 (0.1198)	1670 (0.0584)	1968 (0.0417)
data/restraints/param.	1469/0/127	2288/0/228	1551/0/164	1968/0/190
goodness-of-fit on F^2	1.065	1.082	1.63	1.031
R_1/wR_2 $[I > 2\sigma(I)]$	0.0503/0.1260	0.0496/0.1263	0.0485/0.0722	0.0437/0.1051
R_1/wR_2R (all data)	0.0639/0.1406	0.0525/0.1269	0.0510/0.0734	0.0550/0.1122
largest diff. peak/hole	0.312/−0.211	0.781/−0.353	0.19/−0.32	0.332/−0.387

and used the riding model and weighting scheme $w = 1/[\sigma^2(F_o^2) + (0.0526P)^2 + 0.4948P]$ where $P = [F_o^2 + 2F_c^2]/3$.[19]

Acknowledgment. We thank Yichun Wang for preliminary work on these reactions, Timothy Clark, Peter A. Petillo, and Martin Saunders for supplying computer programs, the National Institutes of Health (Grant GM 29549) and the National Science Foundation (Grant CHE-9417946) for partial financial support, and the National Science Foundation, National Institutes of Health, and the University of Wisconsin for providing financial support for the instrumentation and computers used.

JO951208J

---

[19] The author has deposited atomic coordinates for **3**, **$3^{\cdot+}$** OTs^{-}, **3** (OAc), and **$1^{\cdot}$**(SPh) with the Cambridge Crystallographic Data Centre. The coordinates can be obtained, on request, from the Director, Cambridge Crystallographic Data Centre, 12 Union Road, Cambridge, CB2 1EZ, UK.